Nuclear Engineering and Design 239 (2009) 1804–1810

Contents lists available at ScienceDirect

Nuclear Engineering and Design

journal homepage: www.elsevier.com/locate/nucengdes

Wavelet-based angular dependence analysis of the heterogeneous calculation on MOX fuel lattice

Youqi Zheng, Hongchun Wu, Liangzhi Cao*

School of Nuclear Science and Technology, Xi'an Jiaotong University, Xi'an, Shaanxi, 710049, China

ARTICLE INFO

Article history:
Received 23 December 2008
Received in revised form 15 May 2009
Accepted 27 May 2009

ABSTRACT

A wavelet-based transport method is developed to satisfy the high order angular approximation, which has been proved to be necessary in the heterogeneous calculation of MOX fuel lattice. Based on the new angular discretization scheme, the angular dependence of flux is analysed to find out the origin of complicated angular anisotropy and its effects on the heterogeneous calculation. Both of the geometric and neutronic effects are investigated quantitatively to find out the angular dependence in heterogeneous calculations. Comparisons between the traditional S_N angular discretization scheme and wavelet-based scheme are analysed to indicate the challenges brought from the MOX fuel lattice heterogeneous calculation. An effective solution is given by using wavelets in the angular discretization of neutron transport equation. Improvements of high order angular approximation are suggested.

1. Introduction

Mixed Oxide (MOX) fuel has been widely used in various types of nuclear reactors because of its excellent performance in the advanced fuel cycles and proliferation resistance. With the rapid expansion of nuclear energy and shortage of nuclear resources, MOX fuel will play a more and more important part in the future. But the utilization of MOX fuel raises some challenges to the reactor physics calculation. One of them comes from the hard neutron spectrum because of the existence of plutonium. Many efforts have been done on the fuel lattice heterogeneous calculation. Adams (2001) found that the angular flux exhibit severely oscillatory distribution in the radial direction. But neither further investigation of this phenomenon nor an efficient solver was suggested. Smith (2001) also found that very high order angular approximation was necessary but it was difficult to converge by using traditional angular discretization schemes. Up to now, however, no further analysis on this phenomenon or effective solution of this difficulty has been found in the literatures.

The key point of heterogeneous calculation is to precisely describe the spatial and angular dependence of neutron flux. The angular variable, which was not considered much in previous investigations, is now attracting more attentions. Previous studies focused on only the aftereffects of the angular anisotropy but suggested no significant improvement except increasing the order of angular discretization. For these reasons, a new method based on the wavelet theory was introduced to discretize the angular variable of neutron transport equation (Cho and Cao, 2006; Cao et al., 2008). It encourages a new angular discretization scheme, which is expected to detect the realistic distribution of angular flux. Furthermore, the wavelets can accurately simulate irregular functions with a relative low computational cost. Based-on this new angular discretization scheme, heterogeneous calculations are performed on the MOX fuel lattice to analyse the angular anisotropy and its effects on the neutron transport solution. Not to compare the differences between homogeneous and heterogeneous calculations, in this paper, we focus on the aftereffect while using the heterogeneous calculation. By investigating the mechanism of challenges encountered in the heterogeneous calculation, we propose to suggest effective solutions to handle the challenges in previous studies.

This paper is organized as follows: a brief introduction of the wavelets and wavelet-based transport method is given in Section 2. Following is the analysis of angular flux distribution and its effect on the MOX fuel heterogeneous calculation in Section 3, together with the analysis on different angular discretization schemes. Finally, in Section 4 the conclusions are given to close the paper.

2. Wavelet-based neutron transport equation

2.1. Fundamental of wavelets

The Daubechies' wavelets (Daubechies, 1992) applied here are constructed by using multi-resolution analysis in vision of decomposition and reconstruction. The idea of a multi-resolution analysis

* Corresponding author at: Department of Nuclear Engineering, Xi'an Jiaotong University, 28 Xianning West Road, Xi'an, Shaanxi, 710049, China.
Tel.: +86 29 8266 3285; fax: +86 29 8266 7802.
E-mail addresses: caoliangzhi@gmail.com, caolz@mail.xjtu.edu.cn (L. Cao).

0029-5493/$ – see front matter © 2009 Elsevier B.V. All rights reserved.
doi:10.1016/j.nucengdes.2009.05.026

is to write an arbitrary function f in $L^2(R)$ as a limit of successive approximations, each of which is a smooth version of f. The successive approximations use different resolution. Eqs. (1)–(3) denote the concept of multi-resolution analysis as:

$$\dots V_{-1} \subset V_0 \subset V_1 \subset V_2 \dots \tag{1}$$

$$\bigcap_{m\in Z} V_m = \{0\},\ \overline{\bigcup_{m\in Z} V_m} = L^2(R) \tag{2}$$

$$f \in V_m \Leftrightarrow f(2\cdot) \in V_{m+1} \tag{3}$$

where V_m is a family of embedded closed subspaces in $L^2(R)$.

The Daubechies' wavelets consist of the wavelet functions and scaling functions. The relationship between them is called two-scale relations such as:

$$\phi(x) = \sum_k c_k \phi(2x-k) \tag{4}$$

and

$$\psi(x) = \sum_k d_k \phi(2x-k) \tag{5}$$

where ϕ and ψ stand for the scaling function and wavelet function, respectively. Daubechies (1992) defined a series of coefficients c_k and d_k, which determined a kind of orthonormal and compactly supported wavelets. Eq. (6) and Eq. (7) formulates the final form of Daubechies' wavelets and the corresponding support regions.

$$\begin{aligned}\phi_{n,k}(x) &= \sum_{j=2k}^{2N+2k-1} c_{j-2k}\phi_{n+1,j}(x) \quad \text{support}\,(\phi_{n,k}(x)) \\ &= [2^{-n}k, 2^{-n}(k+2N-1)]\end{aligned} \tag{6}$$

and

$$\begin{aligned}\psi_{n,k}(x) &= \sum_{j=2k-2N+2}^{2k-1} (-1)^j c_{1-j+2k}\phi_{n+1,j}(x) \quad \text{support}\,(\psi_{n,k}(x)) \\ &= [2^{-n}(k+1-N), 2^{-n}(k+N)]\end{aligned} \tag{7}$$

where c_k is called Daubechies' coefficients. Eq. (8) and Eq. (9) define the orthonormal properties of Daubechies' wavelets, which are important for deducing the wavelet-based neutron transport equation.

$$\int \phi_{n,k}(x)dx = 1, \qquad \int \psi_{n,k}(x)dx = 0 \tag{8}$$

and

$$\int \phi_{n,k}(x)\phi_{m,l}(x)dx = \delta_{mn}\delta_{kl}, \qquad \int \psi_{n,k}(x)\psi_{m,l}(x)dx = \delta_{mn}\delta_{kl} \tag{9}$$

Suppose the scaling function satisfies $\phi \in V_0$, for all $m \in Z$, ϕ_{mn} constitute an unconditional basis for V_m as

$$\overline{V_m = \text{linear span}\{\phi_{mn}, n \in Z\}} \tag{10}$$

Then, the wavelets constitute an unconditional basis for $L^2(R)$, i.e., an arbitrary function f in $L^2(R)$ can be represented as:

$$f(x) = \sum_{k=-\infty}^{\infty} a_k \phi(x-k) + \sum_{j=0}^{\infty}\sum_{k=-\infty}^{\infty} a_{j,k}\psi(2^j x - k) \tag{11}$$

Suppose P_m is the projection operator, $P_m f$ satisfies:

$$\lim_{m\to\infty} P_m f = f \tag{12}$$

The approximate expansion of f is written as:

$$f(x) \approx f_m(x) = \sum_k c_{m,k}\phi_{m,k}(x) \tag{13}$$

Numerical tests have demonstrated that a limit sum of Daubechies' scaling functions can accurately simulate kinds of functions, no matter the simulated function is regular as in Fig. 1(a) or irregular as in Fig. 1(b)–(d). It is very important for the following investigations, which require the wavelets can reconstruct the angular flux as accurately as possible.

2.2. Discretization of neutron transport equation using the wavelets

In this paper, the neutron transport process is described by the original steady linear neutron transport equation such as Eq. (14) for the angular flux $\Phi(r, \Omega, E)$.

$$\begin{aligned}&\Omega\nabla\Phi(r,\Omega,E) + \Sigma_t\Phi(r,\Omega,E) \\ &= q_f(r,\Omega,E) + q_s(r,\Omega,E) + q_{ex}(r,\Omega,E)\end{aligned} \tag{14}$$

where r, Ω and E stands for the spatial, directional and energetic variables, respectively. q_f and q_s are the source items as in Eqs. (15) and (16). q_{ex} denotes the extra source item.

$$q_f(r,\Omega,E) = \frac{\chi(E)}{4\pi k}\int_0^\infty \int_{4\pi} \nu\Sigma_f(\Omega',E')\Phi(r,\Omega',E')d\Omega'dE' \tag{15}$$

$$q_s(r,\Omega,E) = \int_0^\infty \int_{4\pi} \Sigma_s(\Omega'\to\Omega, E'\to E)\Phi(r,\Omega',E')d\Omega'dE' \tag{16}$$

The wavelet-based form of neutron transport equation is derived from the multi-group approximation in a two-dimensional Cartesian geometry. The spatial and angular coordinates in the leakage operator are defined as in Eqs. (17)–(19):

$$\Omega\cdot\nabla = (\Omega_x,\Omega_y)\cdot\left(\frac{\partial}{\partial x},\frac{\partial}{\partial y}\right) = \Omega_x\frac{\partial}{\partial x} + \Omega_y\frac{\partial}{\partial y} \tag{17}$$

$$\Omega_x = (1-\mu^2)^{1/2}\cos\varphi \tag{18}$$

$$\Omega_y = (1-\mu^2)^{1/2}\sin\varphi \tag{19}$$

where μ is the polar cosine in the axial direction and φ is the azimuthal variable in the radial direction. Only isotropic scattering are considered to simplify the deduction and analysis.

A decoupled angular discretization scheme (Cao et al., 2008) is deduced by using S_N scheme in the polar variable and wavelet expansion in the azimuthal variable. As basis functions, the wavelets are applied to simulate the realistic continuous angular flux in the radial direction. The angular discretization scheme starts with the polar integration by using Gaussian quadrature set as

$$\int d\mu \left\{(\Omega\nabla + \Sigma_t)\Phi_g(r,\mu,\varphi) - S_g(r,\mu,\varphi)\right\} = 0 \tag{20}$$

where $\Phi_g(r,\mu,\varphi)$ denotes the angular flux in group g as

$$\Phi_g(r,\mu,\varphi) = \int_{\Delta E_g} \Phi(r,\mu,\varphi,E)dE \tag{21}$$

and $S_g(r,\mu,\varphi)$ denotes the source item for brevity.

Based on the discretized equation as in Eq. (22) and Eq. (23):

$$(\Omega_m\nabla + \Sigma_t)\Phi_{g,m}(r,\varphi) = S_{g,m}(r,\varphi) \tag{22}$$

$$S_{g,m}(r,\varphi) = q_{f,g,m}(r,\varphi) + q_{s,g,m}(r,\varphi) + q_{ex,g,m}(r,\varphi) \tag{23}$$

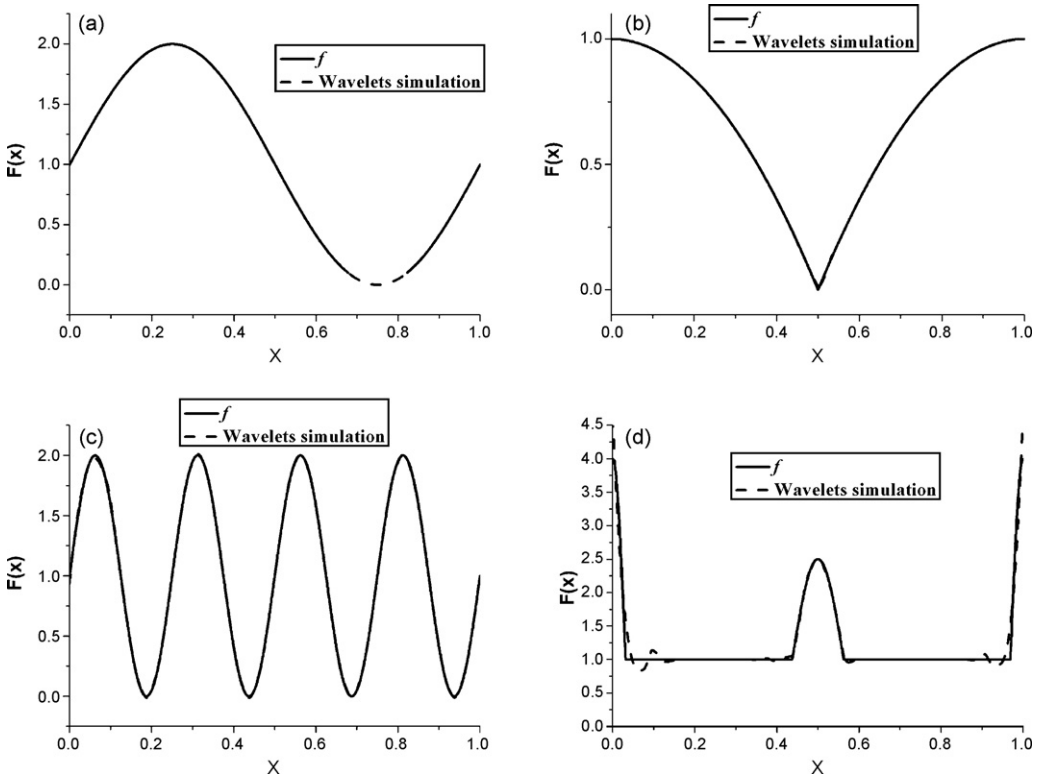

Fig. 1. Simulations of different functions by using the wavelet expansion.

The Daubechies' wavelet expansion is used as in Eq. (24), where the scaling function is applied as the basis function.

$$\Phi_{g,m}(r, \Omega) = \sum_{n=1}^{P} \Psi_{g,mn}(r)\phi_n(\varphi) \tag{24}$$

The Galerkin method is applied to deal with the wavelet expansion coefficients such as

$$\int \phi_{n'}(\varphi)d\varphi \left\{ (\Omega_m \nabla + \Sigma_t) \sum_{n=1}^{P} \psi_{g,mn}(r)\phi_n(\varphi) - S_{g,m}(r, \varphi) \right\} = 0 \tag{25}$$

and the final discretized form of neutron transport equation is given as in Eqs. (26)–(29):

$$\sum_{n=1}^{P} (D_{x,mnn'} \frac{\partial \Psi_{g,mn}}{\partial x} + D_{y,mnn'} \frac{\partial \Psi_{g,mn}}{\partial y}) + \Sigma_t \Psi_{g,mn'} = S_{g,mn'} \tag{26}$$

$$D_{x,mnn'} = (1 - \mu_m^2)^{1/2} \int \cos\varphi \phi_n(\varphi)\phi_{n'}(\varphi)d\varphi \tag{27}$$

$$D_{y,mnn'} = (1 - \mu_m^2)^{1/2} \int \sin\varphi \phi_n(\varphi)\phi_{n'}(\varphi)d\varphi \tag{28}$$

$$S_{g,mn'} = \int \phi_{n'}(\varphi) S_{g,m}(r, \varphi)d\varphi \tag{29}$$

This is a coupled partial difference equation set with only spatial variables. In this paper, the equation set in term of wavelet expansion coefficients are solved by using the finite difference method with diamond approximation.

3. Angular dependence of MOX fuel lattice heterogeneous calculation

A multi-dimensional neutron transport code WAVTRAN was programmed based on the method given above. In this section, it is used to analyse the angular dependence in the MOX fuel lattice heterogeneous calculation. The wavelet-based method is firstly verified by calculating typical UO_2 and MOX fuel cells. In order to find out the mechanism of angular flux distribution and cases in which the strong angular anisotropy appears, the pin cells with different materials are calculated and analysed. Furthermore, the effects of angular anisotropy on the computational accuracy are assessed quantitatively by comparing the results obtained from different angular discretization schemes. The angular flux reconstructions are given by using wavelet expansions to analyse the challenges encountered in the heterogeneous calculations.

In the following calculations, the angular flux reconstructions are applied in the center of lattice for two reasons. Firstly, the fuel center can be supposed as the start of neutron transport process, since the neutron is usually considered to arise inside the fuel and fly out of the cell with or without collision. Secondly, at this point, the incident and emergent neutrons transport in the same path inside the fuel. Therefore, the angular flux here suffers the least effect of geometric anisotropy. Besides, the fast flux attracts most attentions in this paper for its severe and dominative effects.

3.1. Verification of wavelet-based solution

Although the wavelet-based solution has been benchmarked in previous studies (Cao et al., 2008), calculations in a MOX pin cell are performed here to verify the accuracy for heterogeneous calculations. The verifications are performed on four types of pin cells, including a UO_2 fuel and three MOX fuels containing 4.3%, 7.0%, and 8.7% enriched fuel, respectively. The 7-group macro cross-sections are obtained from the literature published by OECD/NEA (Lewis et

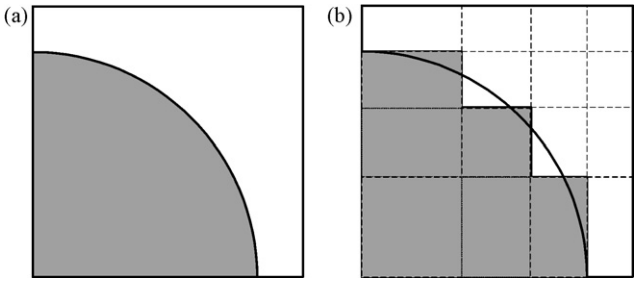

Fig. 2. Geometric descriptions of pin cell lattice (a) original pin cell; (b) 'staircase' approximation for the FDM calculation.

al., 2001), using DRAGON (Marleau et al., 1997) collision probability code and considering fuel-cladding homogenization and moderator.

To use the finite difference method in the spatial discretization of pin cell structure, the circular fuel pin as in Fig. 2(a) was approximated by Cartesian meshes. The meshes are chosen such that the average distance between the circular fuel pin borderline and the 'staircase' approximation is minimized (OECD/NEA, 2003). The approximate meshes are illustrated in Fig. 2(b). A multi-group Monte Carlo method using 10^4 particles and 250 histories is applied to provide the reference solutions. Tables 1–4 give the k_{inf} and its percentage relative error obtained from the wavelet-based solutions. The error decreases with the increase of angular freedom.

3.2. Geometric effects on the angular anisotropy

Traditional neutron transport calculation in the pin cell level is performed by using geometric equivalence, in which the moderator region is transformed to be a concentric annulus and the reflective boundary condition is replaced by the white boundary condition, correspondently. The collision possibility method (CPM) is widely used in such calculations. After geometric equivalence, the angular flux distribution is almost isotropic as illustrated in Fig. 3. Therefore, all traditional methods, even though considering little about the angular anisotropy, are accurate enough in such calculation.

Table 1
k_{inf} and relative error in UO_2 pin cell.

Angular freedom	16	64	256	Reference
k_{inf}	1.32549	1.32558	1.32565	1.32594
Relative error (%)	0.034	0.027	0.022	–

Table 2
k_{inf} and relative error in 4.3% MOX pin cell.

Angular freedom	16	64	256	Reference
k_{inf}	1.13314	1.13470	1.13552	1.13551
Relative error (%)	0.208	0.071	−0.001	–

Table 3
k_{inf} and relative error in 7.0% MOX pin cell.

Angular freedom	16	64	256	Reference
k_{inf}	1.15630	1.15855	1.15967	1.16097
Relative error (%)	0.402	0.208	0.112	–

Table 4
k_{inf} and relative error in 8.7% MOX pin cell.

Angular freedom	16	64	256	Reference
k_{inf}	1.16891	1.17143	1.17272	1.17466
Relative error (%)	0.490	0.275	0.165	–

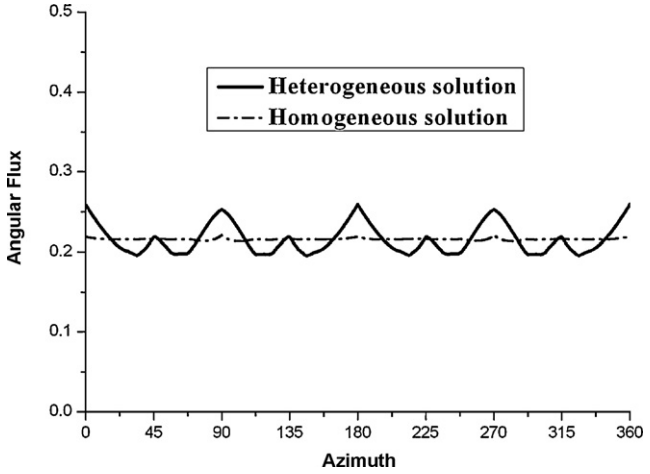

Fig. 3. Comparison of the angular flux distribution between homogeneous and heterogeneous calculations.

However, in case of heterogeneous calculations, the angularly isotropic flux distribution will be replaced by the peaky one for the realistic geometry and reflective boundary condition as illustrated in Fig. 3. Two-dimensional calculation becomes inevitable and corresponding high order angular discretization scheme are necessary in such problem. In this paper, the S_N angular discretization scheme and wavelet-based angular expansion are considered.

Further investigations focus on the origin of peaky angular flux distribution. There are two keys to be analysed. One is the circular-square structure and the other is the reflective boundary condition. The reflective boundary condition determines an infinite duplication all around the cell. Compared with the small size of lattice, the long mean free path of neutron (especially for the fast flux) determines that it might travel across more than one lattice without changing the direction. Therefore, the contributions from outside regions must be considered as an ingredient of angular flux. Based on it, the orthogonal and straight sides with reflective boundary conditions determine that all contributions from outside are anisotropic. For instance, toward the central point, the incident angular flux from neighboring lattice at azimuth $\varphi = 0$ spontaneously possesses the highest intensity for the longest path in fuel region and shortest path in moderator region as illustrated in Fig. 4. The one at $\varphi = 90$ is the same. Moreover, another special azimuth is $\varphi = 45^\circ$. Compared with the one in adjacent angular regions, angular flux in this direction possesses obvious higher intensity due to the

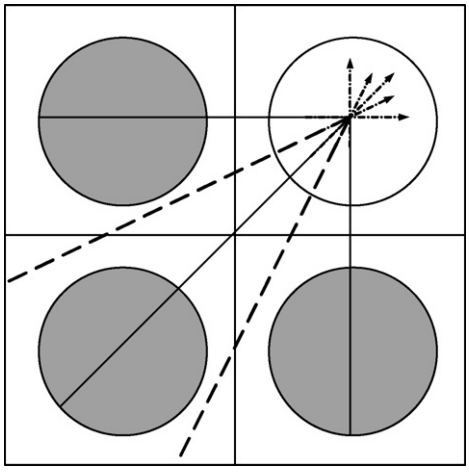

Fig. 4. Geometric effect on the neutron transport process.

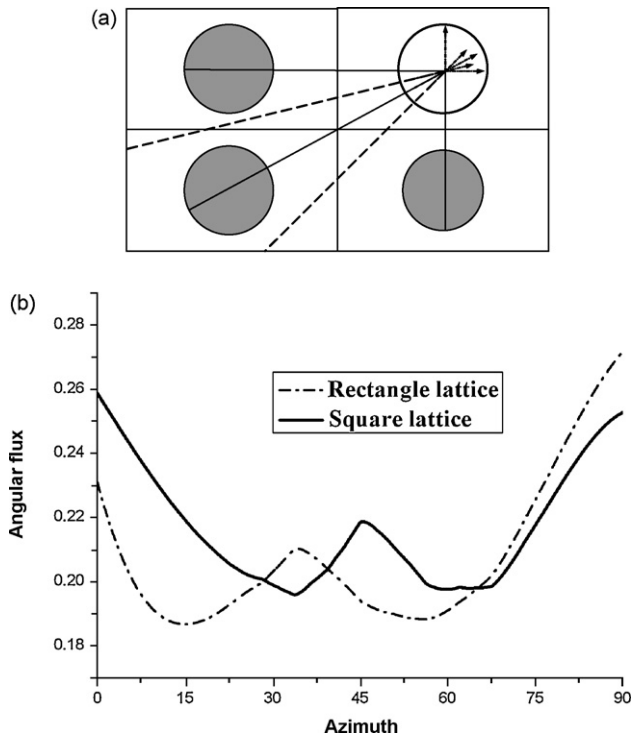

Fig. 5. Differences of the angular flux distribution between different structures (a) rectangle lattice; (b) comparison of angular flux distributions in different lattices.

longest path in fuel region and shorter path in moderator region. Based on it, three peaks arise in the [0, 90] interval of the azimuthal direction as in Fig. 5(b).

In order to verify the reasonability of above analysis, a rectangle problem is calculated as illustrated in Fig. 5(a). In accord with the prediction based on above analysis, the highest peak arises at the azimuth $\varphi = 90$ rather than the ones at both $\varphi = 0$ and $\varphi = 90$ as illustrated in Fig. 5(b). The middle peak is shifted to smaller azimuth due to the varying of lattice. It demonstrates that the peaky distribution of angular flux is essentially determined by the profile of structure and boundary condition.

3.3. Neutronic effects on the angular anisotropy of heterogeneous calculation

Besides the geometric effects on the angular anisotropy, the neutronic effects focusing on the macro cross-section and neutron spectrum are analysed in this section. By using the wavelet-based solution, we reconstruct the angular flux distributions in the center of fuel lattice. The fuels with different materials and enrichment are considered in the reconstructions. The angular flux distributions are illustrated in Fig. 6. Obviously, as in Fig. 6(a), the peaky angular flux distribution of the fast flux (in 1st group) arises. Differences between different fuels arise in two aspects. One is the amplitude of peaks and the other is the different absolute value of angular flux. Both of them are independent with geometric reasons, which suggest us to analyse the neutronic differences between different fuels. Also, the angular flux distribution in the thermal (7th) group is given in Fig. 6(b). Compared with the one of fast flux, the angular distribution of thermal flux is much more smooth and continuous for the frequent collision between nuclei. Such distribution does not require complicated angular approximation and contribute less to the angular anisotropy. Therefore, we focus the investigations on fast flux.

The analysis starts with the comparisons of macro cross-section between fuels. Fig. 7 illustrates the variation of macro absorption

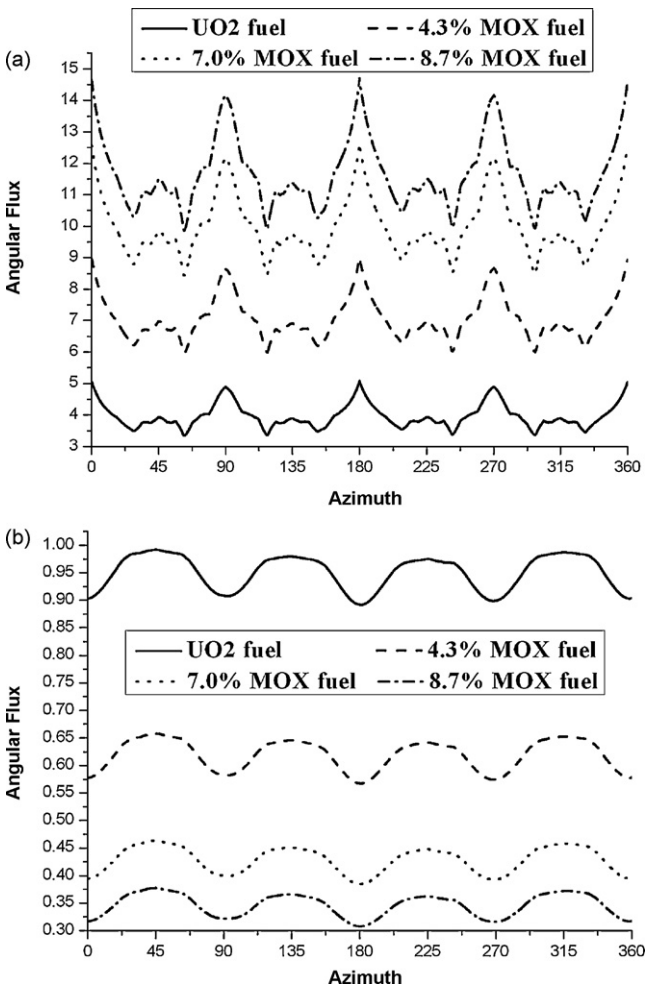

Fig. 6. Angular flux distributions in different fuels (a) fast flux (in the 1st group); (b) thermal flux (in the 7th group).

cross-sections in the fast (1st) group of different fuels. Obviously, the absorption of fast neutron increases with the growth of enrichment. More than 18% increase arises from the UO_2 fuel to the highest enriched MOX fuel. Higher absorption significantly decreases the fast flux from far cells but affect little on the one from neighbors. Therefore, it results higher anisotropy reflected on the amplitude of peaks.

Fig. 8 illustrates the variation of macro fission cross-section in different fuels. Spontaneously, higher enriched MOX fuel cell pos-

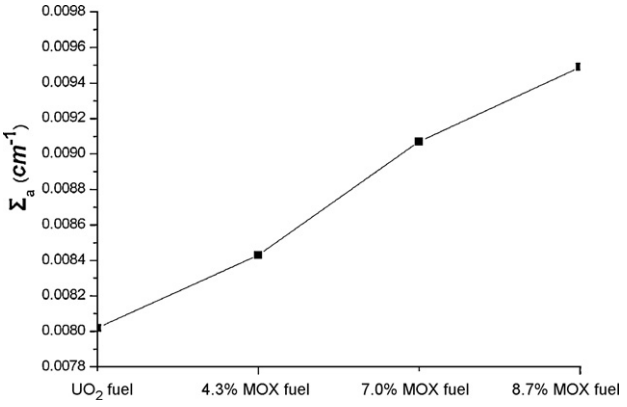

Fig. 7. Variation of the absorption cross-section in the fast (1st) group.

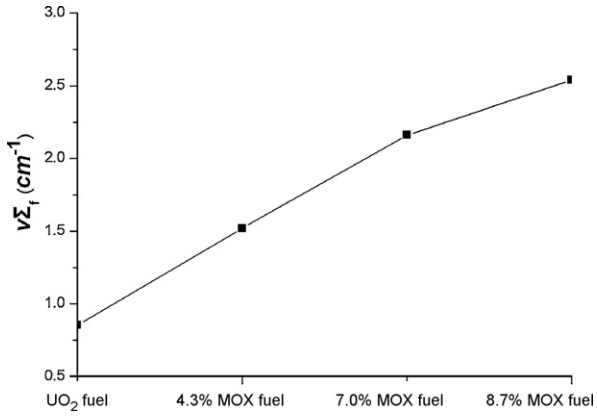

Fig. 8. Variation of the fission cross-section.

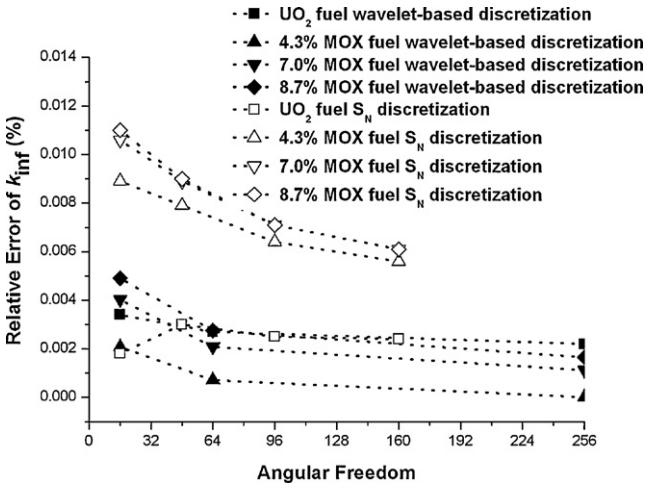

Fig. 11. Changes of the relative error of k_{inf} with the increase of angular freedom.

sesses higher fission rate, which raises higher fast flux. As a result, higher absolute value of flux arises, which is more sensitive to the peaks.

Fig. 9 gives the comparison of macro absorption cross-section between different groups. Significant differences arise in the thermal group, where the higher enriched MOX fuel suffers higher thermal absorption and possesses harder neutron spectrum as illustrated in Fig. 10. And the harder neutron spectrum determines more contributions from fast flux to the final solution.

Anyway, the higher fast neutron absorption determines more severe peaks in the angular flux distribution and the higher fission rate make the flux more sensitive about the peaks. Furthermore, such phenomena are enhanced by the harder neutron spectrum of MOX fuels. Therefore, the MOX fuel lattice heterogeneous calculation suffers severe angular anisotropy inevitably and requires higher order angular approximation.

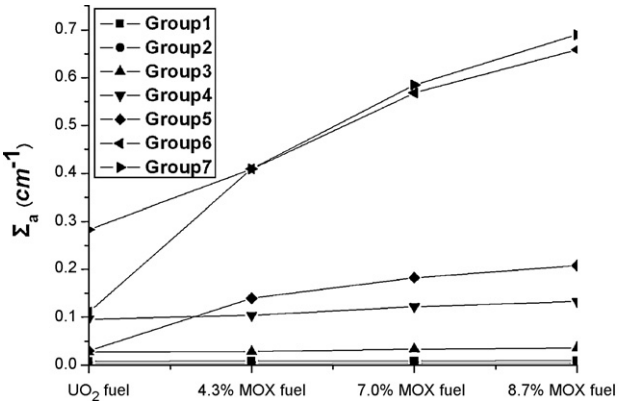

Fig. 9. Comparison of the absorption cross-section.

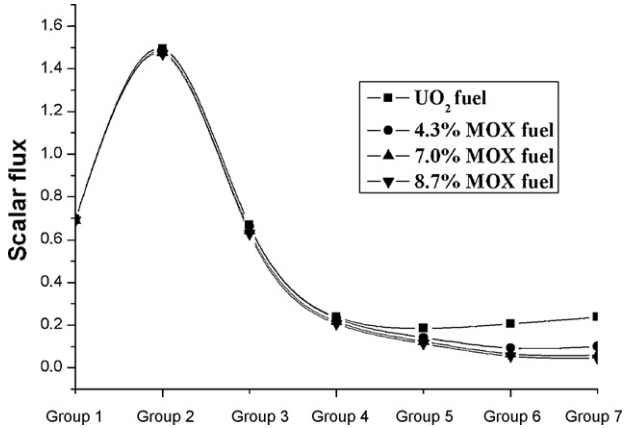

Fig. 10. Comparison of the neutron spectrum.

3.4. Contributions of angular dependence to the computational accuracy

In this section, a series of heterogeneous calculations are performed by using the wavelet-based solution in different fuel cells, including the UO_2 fuel and different enriched MOX fuels. An S_N method DOT IV (Rhoades and Mynatt, 1979) is employed to compare the differences. In order to quantitatively evaluate the effect of angular anisotropy on the heterogeneous calculation, the k_{inf} solutions are compared by using the two angular approximation schemes, i.e., the S_N discretization and wavelet expansion.

Firstly, the changes of relative error of the k_{inf} are given as in Fig. 11. Significant differences arise between the calculations in different fuel cells. Obviously, in the UO_2 fuel, almost no changes arise with the increasing angular freedom, i.e., low order angular approximation is enough in this fuel. However, larger error arises in the calculations of MOX fuels with the increasing enrichment and essential changes arise with the increase of angular freedom. In the MOX fuels, high order angular approximation becomes necessary.

In order to investigate the fundamental of the differences, angular flux reconstructions by using high order (S_{16}) and low order (S_8) S_N approximations are given in Fig. 12, considering the UO_2 fuel and highest enriched fuel. In the fast (1st) group, no obvious differences arise between the UO_2 fuel cell and MOX fuel in low order approximation. But oscillation arises in the MOX fuel in high order approximation. In the thermal (7th) group, however, smooth angular flux distributions are well satisfied by using both different order S_N approximations. It demonstrates the reasonability of investigations on only fast flux.

The fitting S_{16} angular flux reconstructions are compared with the continuous reconstruction by using the wavelet-based solution. As illustrated in Fig. 13, the angular flux in the azimuthal direction agrees well with each other by using different angular discretization schemes. However, due to the peaky angular flux distribution, the S_N scheme becomes worse while the peaks become more severe. It is due to the loss of quadrature points in the peaks. Differing from the S_N method, the wavelet-based solution represents the peaks locally and contains most information about the angular flux distribution. It is the reason that the wavelet-based solutions exhibit better precision in such problem.

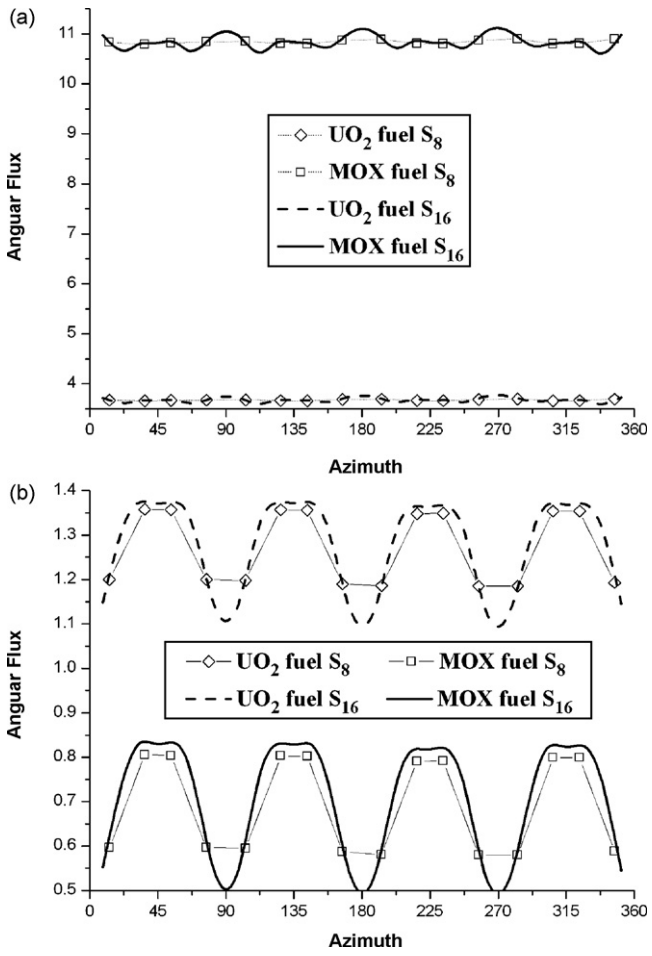

Fig. 12. Comparison of the angular flux reconstructions with different S_N order (a) 1st group; (b) 7th group.

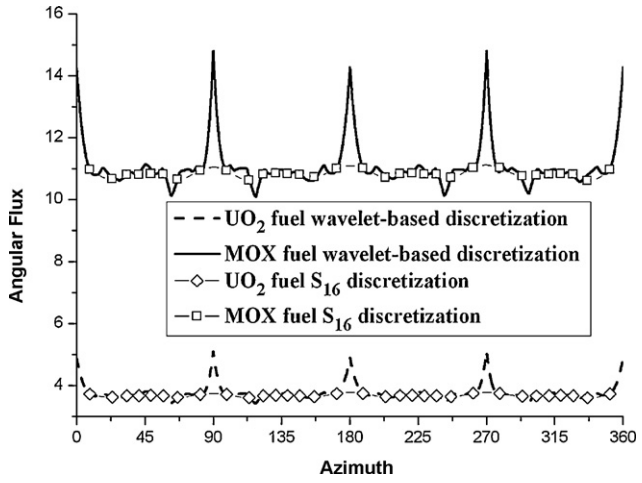

Fig. 13. Comparison of the angular flux reconstructions between different angular discretization schemes.

4. Conclusions

This paper focuses on the heterogeneous calculation of MOX fuel lattice in different cases. Due to the direct calculation considering realistic geometry and reflective boundary condition, a peaky angular flux distribution arises. Both of the geometric and neutronic effects are analysed. Then the effects of peaky angular flux distribution on the MOX fuel lattice heterogeneous calculations are investigated.

The peaky distribution of angular flux arises corresponding to the heterogeneous calculations in a pin cell structure with the reflective boundary condition. In the lattice, neutron flies into or out of the pin cell with different length of path. Based on it, the long mean free path of neutron and reflective boundary condition bring different contributions from different directions to the angular flux. Therefore, the peaky distribution arises, especially for the fast flux, whose mean free path is long enough. With the increase of absorption, such peaky performance of angular flux will be enhanced, since the contributions from far cells are lessened. It is just encountered in the pin cell heterogeneous calculations. Furthermore, in the MOX fuels, higher fission rate and harder neutron spectrum make the effect of peaky angular flux distribution more severe. It determines that high order angular approximation is necessary in such problem. Further analysis indicates that the traditional high order angular approximation such as the S_N approximation seems no longer as effective as before. It is caused by the loss of angular quadrature points in the peaks.

Potential developments in the MOX fuel lattice heterogeneous calculation are suggested based on the analysis above. Firstly, for S_N angular approximation, a suitable azimuthal quadrature set is very important. Better options, which suffer less sensitivity about the peaks, might significantly improve the accuracy with refinements. Secondly, special determinations of the angular flux distribution corresponding with lattice encourage an idea to develop a new angular approximation scheme based on the peaky performance, e.g., the peak detecting techniques such as the wavelet analysis. Finally, not all calculations require complicated angular approximation for the different geometric and neutronic properties. It encourages many new techniques, such as the angular self-adaptive technique.

Acknowledgement

This research was carried out under the financial support of the National Science Foundation of China (Approved number 10605017 and 10875094).

References

Adams, M.L., 2001. Angular dependence of the fast flux in reactor lattices. Trans. Am. Nucl. Soc. 81, 212–214.

OECD/NEA, 2003. Benchmark on Deterministic Transport Calculations Without Spatial Homogenisation. NEA/NSC/DOC (2003) 16.

Cao, L., Wu, H., Zheng, Y., 2008. Solution of neutron transport equation using Daubechies' wavelet expansion in the angular discretization. Nucl. Eng. Des. 238, 2292–2301.

Cho, N.Z., Cao, L., 2006. Wavelet-theoretic method for solution of neutron transport equation. In: Transactions of the Korean Nuclear Society Spring Meeting, Chuncheon, Korea, May 25–26.

Daubechies, I., 1992. Ten Lectures on Wavelets. SIAM, Philadelphia, PA.

Rhoades, W.A., Mynatt, F.R., 1979. The DOT-IV: Two-Dimensional Discrete Ordinates Transport Code[R]. Oak Ridge National Laboratory, USA.

Lewis, E.E., et al., 2001. Benchmark specification for Deterministic 2-D/3-D MOX fuel assembly transport calculations without spatial homogenization (C5G7 MOX). NEA/NSC/DOC (2001) 4.

Marleau, G., et al., 1997. A User's Guide for DRAGON. Ecole Polytechnique de Montréal.

Smith, M.A., 2001. Comparison of angular approximations for PWR cell calculations. Trans. Am. Nucl. Soc. 84, 90–91.